	1.0		2.8		2.5
			3.2		2.2
			3.6		
	1.1		4.0		2.0
					1.8
	1.25		1.4		1.6

MICROCOPY RESOLUTION TEST CHART
NATIONAL BUREAU OF STANDARDS 1963 A

Prepared for
SPACE DIVISION
AIR FORCE SYSTEMS COMMAND
Los Angeles Air Force Station
P.O. Box 92960, Worldway Postal Center
Los Angeles, California 90009

82 02 01 166

This report was submitted by The Aerospace Corporation, El Segundo, CA 90245, under Contract No. F04701-80-C-0081 with the Space Division, Deputy for Technology, P.O. Box 92960, Worldway Postal Center, Los Angeles, CA 90009. It was reviewed and approved for The Aerospace Corporation by H. E. F. Wang, Principal Director, Space Test Directorate. Lt. Col. J. Durrett, YLS, was the Director, Space Sensor Test Directorate for the Deputy of Technology.

This technical report has been reviewed and is approved for publication. Publication of this report does not constitute Air Force approval of the report's findings or conclusions. It is published only for the exchange and stimulation of ideas.

FOR THE COMMANDER

J. Durrett, Lt. Col., USAF
Director
Space Sensor Test Directorate
Deputy of Technology

REPORT DOCUMENTATION PAGE		READ INSTRUCTIONS BEFORE COMPLETING FORM
1. REPORT NUMBER SD-TR-81-93	2. GOVT ACCESSION NO. AD-A112 396	3. RECIPIENT'S CATALOG NUMBER
4. TITLE (and Subtitle) MULTI-BODY GIMBAL SERVO SYSTEM SIMULATION MODEL		5. TYPE OF REPORT & PERIOD COVERED Final
		6. PERFORMING ORG. REPORT NUMBER TR-0082(2757-01)-1
7. AUTHOR(s) P. R. Dahl		8. CONTRACT OR GRANT NUMBER(s) F04701-80-C-0081
9. PERFORMING ORGANIZATION NAME AND ADDRESS The Aerospace Corporation El Segundo, California 90245		10. PROGRAM ELEMENT, PROJECT, TASK AREA & WORK UNIT NUMBERS P.E. 62301E
11. CONTROLLING OFFICE NAME AND ADDRESS Space Division Air Force Systems Command Los Angeles, Calif. 90009		12. REPORT DATE 10 December 1981
		13. NUMBER OF PAGES 44
14. MONITORING AGENCY NAME & ADDRESS(if different from Controlling Office)		15. SECURITY CLASS. (of this report) Unclassified
		15a. DECLASSIFICATION/DOWNGRADING SCHEDULE

16. DISTRIBUTION STATEMENT (of this Report)

Approval for public release; distribution unlimited

17. DISTRIBUTION STATEMENT (of the abstract entered in Block 20, if different from Report)

18. SUPPLEMENTARY NOTES

19. KEY WORDS (Continue on reverse side if necessary and identify by block number)

Multi-Body Dynamics, Gimbal Servo System,
Multi-Body Control System, Simulation of a Gimbal,
Model of a Multi-Body System.

20. ABSTRACT (Continue on reverse side if necessary and identify by block number)

The equations of motion of a multi-body gimbal servo system for simulation
purposes are derived using a free body momentum formulation that is maintained
throughout the development, thereby retaining the original variables defined
in the beginning of the model formulation. By avoiding undesirable algebraic
manipulation and transformation of the original variables, a simplification is
achieved in evolving and understanding a complex computer simulation model
that can be debugged and run with enhanced insight to the physical process
being simulated.

DD FORM 1473
(FACSIMILE)

19. KEY WORDS (Continued)

20. ABSTRACT (Continued)

In the formulation, translational motion is permitted for each gimbal frame, but a translational momentum conservation constraint for the system of "rigidly" connected bodies is invoked to avoid solution of translational equations of motion for each body.

A four-body example is presented where the bodies are simply connected in a series configuration, such as would represent a spacecraft with controlled gimballed appendages.

CONTENTS

1/2

FIGURES

1. INTRODUCTION

Connected multi-body dynamics problems of all kinds have been encountered since the invention of the wheel and its application to a moving platform. The precise formulation of the equations of motion for more than two connected bodies brought little attention, except for the compound pendulum, until the space age, probably because techniques and means for the solution to the equations for two bodies with more than one or two degrees of freedom were generally unavailable or too unwieldy and impractical to use. In the last two decades, tremendous advances have been made in both the formulation methods and computer solution to multi-body/multi-degree of freedom problems. Today, it is not uncommon to obtain computer solutions for multi-body systems including flexible modes with more than twenty degrees of freedom or more than fifty state variables. Even so, such computer programs evolve to usefulness only after the problem equations formulation, computer coding of the equations, and debugging of the problem. The general effectiveness of the resulting multi-body dynamics and control simulation is usually assessed in terms of the formulation and coding and debugging effort, the computer run time, the ease of an analyst to become familiar with the program after it has been developed, and the ease of modifying the program to reflect changes and additions to the design of the system. With these ideas in mind, the multi-body dynamics formulation for a spaceborne gimbal system was undertaken anew.

The approach initially favored was one wherein the "primitive"[1]* Newtonian/Eulerian equations for translational and rotational motion are retained throughout. This would have required retention of all 6 degrees of freedom for each body and the necessity of integrating more state variable equations than are actually needed. Because computer run time is roughly proportional to the number of state variables and to the highest frequency

---

*We use Jerkovsky's definition: By "primitive" equations and variables, we mean equations and variables that refer to each body as a separate and distinct body without regard to how it fits into the multi-body configuration.

5

mode in the system, we can reduce run time considerably by reducing the degrees of freedom of each body to 3 by not solving the translational equations of motion by integration. However, holonomic constraint equations, which are essentially algebraic, that constrain the gimbal geometry to conserve translational momentum of the gimbal system, have been introduced in this paper which supplant the translational differential equations of motion. This is basically the approach initially taken by Russell[2] in his so-called "primed momentum" formulation method. We are then left with 3 rotational degrees of freedom for each body which are permitted for each axis of a Cartesian coordinate frame associated with that body. The Cartesian reference frames are retained from the beginning in order to permit insight, visibility, and a feel for what is dynamically happening throughout the formulation and simulation. Generalized coordinates formulations such as are used in Lagrange, D'Alembert, Hamilton Boltzmann-Hamel, Gibbs, and Kane[3] derivations of the equations of motion are avoided on purpose as is the transformation operator formalism of Jerkovsky.[1,4] This is because a) insight seems to get lost, and b) either hand reduction by matrix inversion of the constraint equations to reduce computer solution time is needed, or this problem is left to the computer whereby run time suffers due to matrix inversions that are performed in each integration step. These other approaches admittedly have the potential of shorter computer run times than are obtained using a momentum formulation because they reduce the number of degrees of freedom for each body to an absolute minimum, e.g., the equations for a single bearing axis gimballed body only needs one degree of "free" rotational freedom, the other two degrees of relative freedom being "hard" constrained or completely nulled via constraint equations.

In the alternative approach taken here, relative motion about the constrained motion axes of the Cartesian frames is permitted, but only slightly. The small to infinitesimal relative motions allowed require additional solutions of angular motions transverse to the bearing axis but we eliminate the need for hand or computer solution of "hard" constraint equations which generally involve matrix inversions. An advantage obtained is that the true transverse axis dynamics can be revealed and their effect on

6

system stability evaluated. However, because gimbal bearing transverse axis stiffnesses can be large, the highest associated eigenvalue frequency can be considerably higher than the highest control loop component bandwidth thereby requiring shortening of the integration step size merely to get the constraint satisfied. This shortcoming can be alleviated after one ascertains that high frequency mode instability is not a problem by artificially reducing transverse axis stiffness or increasing transverse axis viscous friction in a way that lowers the transverse axis characteristic frequency to the vicinity of the control loop bandwidths.

The multi-body equations presented in this paper are derived for bodies in an open chain tree[5] configuration typical of a spacecraft with two or more gimballed elements. The rotational equations of motion of one of the bodies are general for open chain tree configurations as are the translational momentum constraint equations. The equations and matrix-scalar block diagrams are given for an example 4-body system comprised of a 3 axis controlled spacecraft, a single axis controlled solar array, and a 2-axis gimbal controlled payload with a gimbal yoke that has mass and inertia.

2. GIMBALLED BODY MOMENTUM

Referring to Figure 1, we imagine the gimballed body with a mass element dm at $\vec{R}$ relative to an inertial frame I to be gimballed about one of the axes of a frame G whose basis vectors are parallel to those of frame g at the c.m. of the body. Frame g is displaced an amount $\vec{r}_1$ from the frame G and both frames are fixed in the body and therefore rotate with the body at its inertial angular rate $\vec{\omega}$. Then the moment of momentum of this body about the origin of the frame g, or in other words, about its center of mass is[5-8]

$$\vec{H}_g = \int \vec{r} \times \dot{\vec{R}} \, dm \tag{1}$$

$$= \int \vec{r} \times (\dot{\vec{R}}_1 + \vec{\omega} \times \vec{r}) dm \tag{2}$$

$$\vec{H}_g = \int \vec{r} \times (\vec{\omega} \times \vec{r}) dm - \dot{\vec{R}}_1 \times \int \vec{r} \, dm \tag{3}$$

The first term on the right side of (3) is $\bar{\bar{I}}_g \cdot \vec{\omega}$ where $\bar{\bar{I}}_g$ is the inertia dyadic or inertia matrix with respect to the frame g, and the integral in the second term is equal to the gimballed body mass M times the radius vector from the frame g to the c.m. which is the null vector and hence is zero. Thus (3) is written as

$$\vec{H}_g = \bar{\bar{I}}_g \cdot \vec{\omega}_g \tag{4}$$
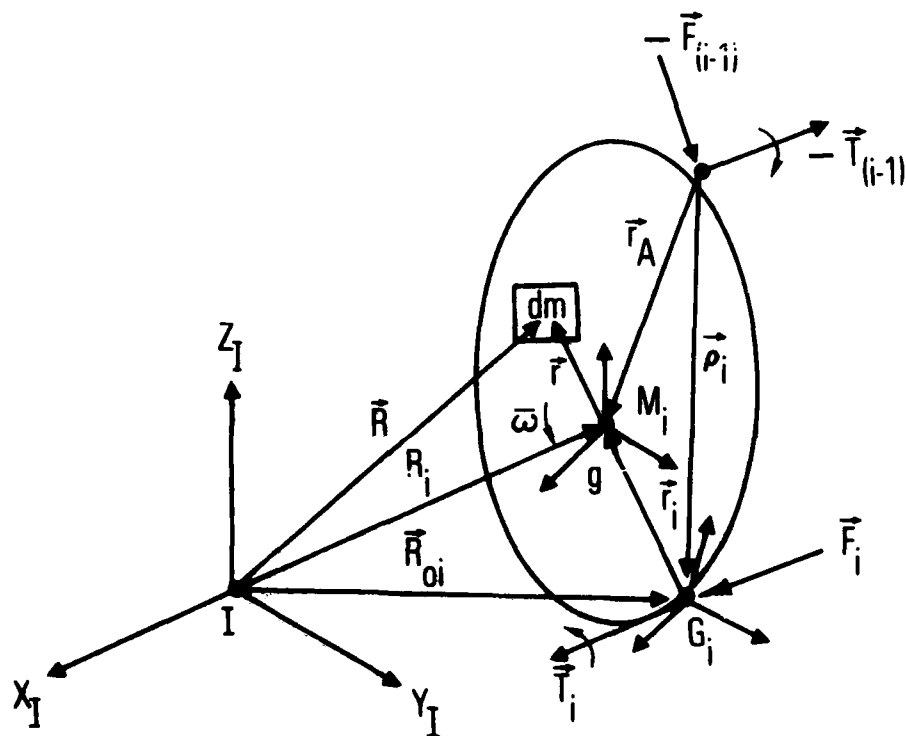
Figure 1. Model of the ith Body

10

3. EQUATIONS OF MOTION

The equation of translational motion for the gimballed body of Figure 1 is

$$M_i \ddot{\vec{R}}_i = \vec{F}_i - \vec{F}_{(i-1)} \tag{5}$$

In the figure, we have assumed two gimbal points on the ith body. The subscript $\underline{i}$ identifies the gimbal frame associated with that body and the interbody force and torque at that point, whereas the subscript $\underline{(i-1)}$ identifies the adjacent connected body and its associated gimbal that it shares with the ith body and its interbody force and torque. The negative of the interbody force and torque acting on the $(i-1)$ body are felt by reaction on the ith body.

The equation of rotational motion about the point g, or center of mass of the body is[5-8]

$$\vec{T}_T - \vec{r}_Q \times \vec{F}_Q = \dot{\vec{H}}_g \tag{6}$$

where

$$\vec{T}_T = \vec{T}_i - \vec{T}_{(i-1)} \tag{7}$$

and

$$\vec{r}_Q \times \vec{F}_Q = (\vec{r}_i \times \vec{F}_i) - \left(\vec{r}_{Ai} \times \vec{F}_{(i-1)} \right) \tag{8}$$

where the last expression has been introduced for convenience in simplifying the form of the resulting equations. In the usual approach we would substitute appropriate combinations of (5) into (8) which process is lengthy and replete with terms. To show the general idea of the equation development, we further simplify by introducing

$$M_Q \ddot{\vec{R}}_Q = \vec{F}_Q \qquad (9)$$

so that

$$\vec{r}_Q \times \vec{F}_Q = \vec{r}_Q \times M_Q \ddot{\vec{R}}_Q \qquad (10)$$

Following the concept introduced by Russell[2] we write (10) as

$$\vec{r}_Q \times \vec{F}_Q = \frac{d}{dt}(\vec{r}_Q \times M_Q \dot{\vec{R}}_Q) - \dot{\vec{r}}_Q \times M_Q \dot{\vec{R}}_Q \qquad (11)$$

Employing (11) in (6) we have

$$\vec{T}_T = \dot{\vec{H}}_g + \frac{d}{dt}(\vec{r}_Q \times M_Q \dot{\vec{R}}_Q) - \dot{\vec{r}}_Q \times M_Q \dot{\vec{R}}_Q \qquad (12)$$

The vector derivatives indicated in (12) are relative to an inertial reference. In order to solve a vector differential equation computationally, it needs to be scalarized in a convenient frame of reference (see Appendix). We wish to use the frame G in our computations and so we find the components of the inertial vector derivatives of $\vec{H}_g$ and $\vec{r}_Q$ which have their bases in that rotating frame. Using Appendix formula (A-15) and scalar component matrix notation,

$$\dot{\bar{H}}_{gI} = \dot{\bar{H}}_{gG} + \bar{\omega}_G \times \bar{H}_{gG} \qquad (13)$$

$$\dot{\bar{r}}_{QI} = \dot{\bar{r}}_{QG} + \bar{\omega}_G \times \bar{r}_{QG} \qquad (14)$$

Because the position vectors in (8) are fixed in the body fixed frame G, $\dot{\bar{r}}_{QG} \equiv 0$.

The vectors $\vec{T}_T$ and $\dot{\vec{R}}_Q$ may have been originally known and expressed in terms of their components in an inertial frame I, however their components in the G frame are straightforwardly obtained by transforming the vector components from the inertial frame I to the gimbal frame G as required, e.g.,

$$\bar{T}_{TG} = \bar{\bar{C}}_I^G \cdot \bar{T}_{TI} \qquad (15)$$

and

$$\dot{\bar{R}}_{QG} = \bar{\bar{C}}_I^G \cdot \dot{\bar{R}}_{QI} \qquad (16)$$

We now employ (13) and (14) in (12) to obtain the matrix-scalar equation expressed in the G frame.

$$\bar{T}_{TG} = \dot{\bar{H}}_G + \bar{\omega}_G \times \bar{H}_G + \frac{d}{dt}(\bar{r}_Q \times M_Q \dot{\bar{R}}_Q)_G$$
$$+ \bar{\omega}_G \times (\bar{r}_Q \times M_Q \dot{\bar{R}}_Q) - (\bar{\omega}_G \times \bar{r}_{QG}) \times M_Q \dot{\bar{R}}_{QG} \qquad (17)$$

where

$$\bar{H}_G \equiv \bar{H}_{gG} = \left(\bar{\bar{I}}_g \cdot \bar{\omega}_g \right)_G = \bar{\bar{I}}_g \cdot \bar{\omega}_G$$

because the frame g is parallel to the frame G. Equation (7) can be written as

$$\bar{T}_{TG} = \dot{\bar{H}}_{PG} + \bar{\omega}_G \times \bar{H}_{PG} - \bar{T}_Q \qquad (18)$$

where

$$\bar{H}_{PG} = \bar{H}_G + \bar{H}_Q \qquad (19)$$

and

$$\bar{H}_Q \equiv \bar{r}_Q \times M_Q \dot{\bar{R}}_Q \qquad (20)$$

13

and

$$\overline{T}_Q = (\overline{\omega} \times \overline{r}_Q) \times M_Q \dot{\overline{R}}_Q \qquad (21)$$

The quantity $\overline{H}_{PG}$ is defined as Russell's[2] "primed" angular momentum, which includes the momentum $\overline{H}_G$ due to rotation about the center of mass plus a term $\overline{H}_Q$ resulting from the translational motion of the body center of mass due to gimballing. The $\overline{H}_Q$ term is referred to as the "swing" momentum.

The term T_Q in (18) is a torque that is related to the acceleration term $(\overline{\omega}_G \times \overline{r}_{QG}) \times \dot{\overline{R}}_{QG}$ and is referred to as the "swing" torque. The swing torque and the time derivative of the swing momentum comprise the interbody torque, i.e., the net torque acting on the ith body due to motion of the ensemble of bodies.

Equations (18) and (19) are the equations describing the angular motion of one of the gimballed bodies in a multi-body system. The solution to these equations is depicted in block diagram form in Figure 2 where $\overline{T}_T$, $\overline{T}_Q$ and $\overline{H}_Q$ are regarded as independent variable inputs in the figure and the computed components $\overline{\omega}_G$ of $\vec{\omega}$ in the gimbal frame G are the output. The inverse $\overline{\overline{I}}_g^{-1}$ of the inertia matrix $\overline{\overline{I}}_g$ which is determined relative to the frame g is a physical parameter as are the mass M and the components of $\overline{r}_Q$ in the gimbal frame. Equations (18) and (19) further simplify to familiar forms if $\vec{r}_Q = 0$ or if $\vec{R}_Q = 0$ which makes the center of mass inertially fixed. The terms $\overline{H}_Q$ and $\overline{T}_Q$ generally will not be zero in a multi-body system and the presence of $\vec{R}_Q$ which is related to the gimballed mass velocity contributes in some cases very significantly to the angular momentum of the body and therefore is very important to consider. Its effect is amplified by the vector $\vec{r}_Q$ which is related to the distance from the gimbal points to the center of mass of the body.

14
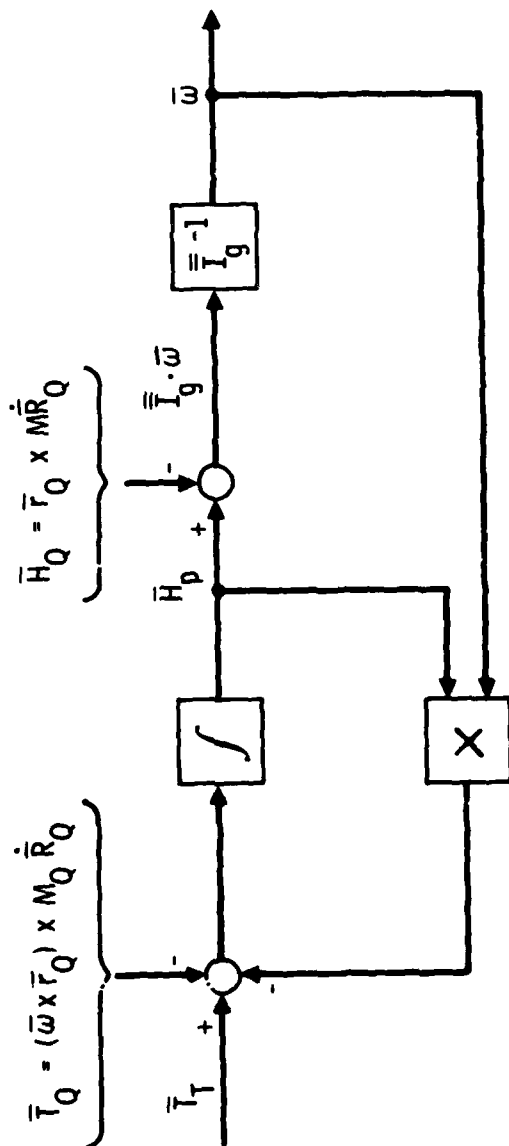
Figure 2. Single Gimballed Body Equation of Motion

4. FOUR BODY SYSTEM DYNAMICS

The translational equations of motion given by (5) are written out, for example, for the four body chain configuration shown in Figure 3,

$$M_1 \ddot{\vec{R}}_1 = \vec{F}_1 \tag{22}$$

$$M_2 \ddot{\vec{R}}_2 = \vec{F}_2 - \vec{F}_1 \tag{23}$$

$$M_3 \ddot{\vec{R}}_3 = \vec{F}_3 - \vec{F}_2 \tag{24}$$

$$M_4 \ddot{\vec{R}}_4 = -\vec{F}_3 \tag{25}$$

4.1 INTERBODY TORQUES

The interbody torques resulting from interbody forces are now determined. It is easily seen that equations (8) and (5) or equations (22-25) yield for the ith body in the chain

$$
\begin{aligned}
\vec{r}_{Qi} \times \vec{F}_{Qi} &= \vec{r}_i \times \sum_{k=1}^{i} M_k \ddot{\vec{R}}_k - \vec{r}_{Ai} \times \sum_{k=1}^{(i-1)} M_k \ddot{\vec{R}}_k \\
&= \vec{r}_i \times M_i \ddot{\vec{R}}_i - \vec{\rho}_i \times \sum_{k=1}^{(i-1)} M_k \ddot{\vec{R}}_k \\
&= \frac{d}{dt} \left[\vec{r}_i \times M_i \dot{\vec{R}}_i - \vec{\rho}_i \times \sum_{k=1}^{(i-1)} M_k \dot{\vec{R}}_k \right] \\
&\quad - \left[\dot{\vec{r}}_i \times M_i \dot{\vec{R}}_i - \dot{\vec{\rho}}_i \times \sum_{k=1}^{(i-1)} M_k \dot{\vec{R}}_k \right]
\end{aligned}
\tag{26}
$$

17

Figure 3. Four-Body System

18

where

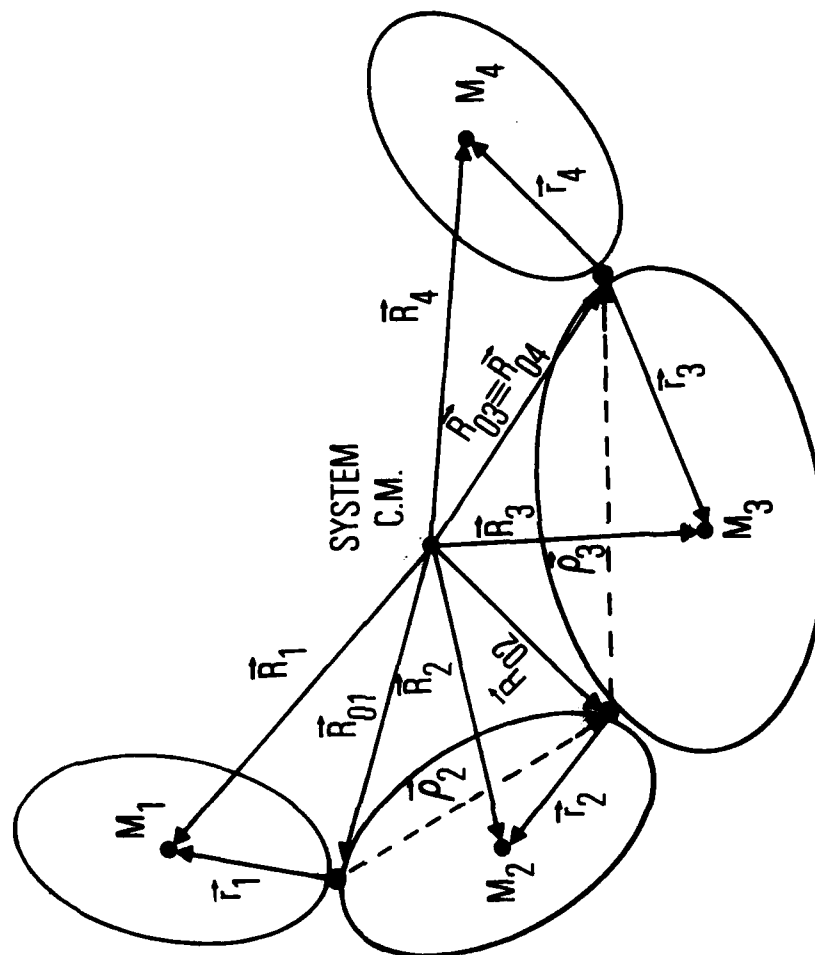$$\vec{\rho}_i = \vec{r}_{Ai} - \vec{r}_i \qquad (27)$$

Comparing (26) with corresponding terms in (17) and (18) it is apparent that the first term in (26) is after scalarizing to the ith gimbal frame

$$\overline{H}_{Qi} = \overline{r}_i \times M_i \dot{\overline{R}}_i - \overline{\rho}_i \times \sum_{k=1}^{(i-1)} M_k \overline{\overline{C}}_k^i \cdot \dot{\overline{R}}_k \qquad (28)$$

where as in (20) we have defined the quantity $\overline{H}_Q$ as the swing momentum term $(\overline{r}_Q \times M_Q \dot{\overline{R}}_Q)$. In particular for the four body chain of Figure 3, using (28) we obtain,

$$\overline{H}_{Q1} = \overline{r}_1 \times M_1 \dot{\overline{R}}_1 \qquad (29)$$

$$\overline{H}_{Q2} = \overline{r}_2 \times M_2 \dot{\overline{R}}_2 - \overline{\rho}_2 \times M_1 \overline{\overline{C}}_1^2 \cdot \dot{\overline{R}}_1 \qquad (30)$$

$$\overline{H}_{Q3} = \overline{r}_3 \times M_3 \dot{\overline{R}}_3 - \overline{\rho}_3 \times (M_1 \overline{\overline{C}}_1^3 \cdot \dot{\overline{R}}_1 + M_2 \overline{\overline{C}}_2^3 \cdot \dot{\overline{R}}_2) \qquad (31)$$

or

$$\overline{H}_{Q3} = \overline{r}_3 \times M_3 \dot{\overline{R}}_3 - \overline{\rho}_3 \times M_4 \overline{\overline{C}}_4^3 \cdot \dot{\overline{R}}_4 \qquad (32)$$

$$\overline{H}_{Q4} = \overline{r}_4 \times M_4 \dot{\overline{R}}_4 \qquad (33)$$

The second term in (26) is the swing torque

$$\vec{T}_{Qi} = \left[\vec{r}_i \times M_i \dot{\vec{R}}_i - \vec{\rho}_i \times \sum_{k=1}^{(i-1)} M_k \dot{\vec{R}}_k \right] \qquad (34)$$

19

which becomes after scalarizing to the ith gimbal frame,

$$\bar{T}_{Qi} = (\bar{\omega}_i \times \bar{r}_i) \times M_i\dot{\bar{R}}_i - (\bar{\omega}_i \times \bar{\rho}_i) \times \sum_{k=1}^{(i-1)} M_k C_k^i \dot{\bar{R}}_k \tag{35}$$

For the four-body system of Figure 3, the swing torques on each body are found to be

$$\bar{T}_{Q1} = (\bar{\omega}_1 \times \bar{r}_1) \times M_1\dot{\bar{R}}_1 \tag{36}$$

$$\bar{T}_{Q2} = (\bar{\omega}_2 \times \bar{r}_2) \times M_2\dot{\bar{R}}_2 - (\bar{\omega}_2 \times \bar{\rho}_2) \times M_1\bar{\bar{C}}_1^2 \cdot \dot{\bar{R}}_1 \tag{37}$$

$$\bar{T}_{Q3} = (\bar{\omega}_3 \times \bar{r}_3) \times M_3\dot{\bar{R}}_3 - (\bar{\omega}_3 \times \bar{\rho}_3) \times (M_1\bar{\bar{C}}_1^3 \cdot \dot{\bar{R}}_1 + M_2\bar{\bar{C}}_2^3 \cdot \dot{\bar{R}}_2) \tag{38}$$

or

$$\bar{T}_{Q3} = (\bar{\omega}_3 \times \bar{r}_3) \times M_3\dot{\bar{R}}_3 - (\bar{\omega}_3 \times \bar{\rho}_3) \times M_4\bar{\bar{C}}_4^3 \cdot \dot{\bar{R}}_4 \tag{39}$$

$$\bar{T}_{Q4} = (\bar{\omega}_4 \times \bar{r}_4) \times M_4\dot{\bar{R}}_4 \tag{40}$$

We can now proceed with the determination of the $\dot{\bar{R}}_i$ terms in (28) in order to calculate the solution of equations (18) and (19) shown in Figure 2. In the material that follows, the subscripts denote the mass and gimbal numbers. The subscript G has been suppressed and replaced merely with the gimbal number i. The total torque T_{Ti} on body i will be found to be comprised of the torque from the ith gimbal elements (torque motor, bearing friction, etc.) plus the reaction torque from the $(i-1)^{th}$ gimbal elements.

4.2 MOMENTUM - KINEMATIC CONSTRAINTS

Figure 3 schematically shows several bodies connected together. A main body is shown which could be the main part of a spacecraft which has a gimbal system that points a payload, e.g., the main body M_3 could be the spacecraft, M_4 its solar array, M_2 a gimbal, and M_1 the payload. The axes G_1 and G_2 would

20

then be the payload gimbal axes and G_3 the solar array gimbal axis. In the following analysis, the subscript number denotes the gimbal frame number and the associated gimballed body number. Refer to the appendix for definitions of vectors, scalars, matrix-scalar expressions and transformations.

It is obvious that the gimbal points move, i.e., the $\vec{R}_{0i}$ change as the gimballed bodies are articulated. We now proceed to find the $\vec{R}_{0i}$.

The center of mass of the system is chosen as the origin of the inertially fixed reference frame corresponding to the $X_I \ Y_I \ Z_I$ frame in Figure 1. This restricts the analysis in this paper to the situation of no external forces that would cause the system c.m. to undergo translational motion. Pure moments about the system c.m. would be permissible. The definition of the center of mass is employed; i.e.,

$$\sum_{i=1}^{4} M_i \vec{R}_i = 0 \tag{41}$$

If we differentiate (41) we get

$$\sum_{i=1}^{4} M_i \dot{\vec{R}}_i = 0 \tag{42}$$

which is a statement of the conservation of translational momentum of the system. Referring to Figure 3, the following vector relations are found:

$$\vec{R}_1 = \vec{R}_{01} + \vec{r}_1$$

$$\vec{R}_2 = \vec{R}_{02} + \vec{r}_2$$

$$\vec{R}_3 = \vec{R}_{03} + \vec{r}_3$$

$$\vec{R}_4 = \vec{R}_{04} + \vec{r}_4$$

In general, for the chain configuration

$$\vec{R}_i = \vec{R}_{01} + \vec{r}_1 \tag{43}$$

Also,

$$\vec{R}_{02} = \vec{R}_{01} + \vec{\rho}_2$$

$$\vec{R}_{03} = \vec{R}_{02} + \vec{\rho}_3$$

where

$\vec{\rho}_2$ = vector from G_1 to G_2, etc.

so in general

$$\vec{R}_{0i} = \vec{R}_{0(i-1)} + \vec{\rho}_i \tag{44}$$

or

$$\vec{R}_{0i} = \vec{R}_{01} + \sum_{k=2}^{i} \vec{\rho}_k \tag{45}$$

Equations (43) and (44) are depicted in Figures 1 and 3. Differentiating (43), we get for the ith body

$$\dot{\vec{R}}_i = \dot{\vec{R}}_{0i} + \vec{\omega}_i \times \vec{r}_i \tag{46}$$

An $(\vec{\omega}_i \times \vec{R}_{0i})$ term is not present because $\vec{R}_{0i}$ vector is not based in the ith body moving/rotating coordinate frame but rather is based in the inertial frame centered at the system c.m. On the other hand, the $\vec{r}_i$ vector is based and fixed in the ith body frame so that its time derivative is identically zero and the $(\vec{\omega}_i \times \vec{r}_i)$ term arises from the $\vec{\omega}_i$ angular rate of the ith body. Similarly, differentiating (44) and (45) we get

22

$$\dot{\vec{R}}_{0i} = \dot{\vec{R}}_{0(i-1)} + \vec{\omega}_i \times \vec{\rho}_i \tag{47}$$

and

$$\dot{\vec{R}}_{0i} = \dot{\vec{R}}_{01} + \sum_{k=2}^{i} (\vec{\omega}_k \times \vec{\rho}_k) \tag{48}$$

Substituting (48) into (46) and the result into (42) we obtain

$$M\dot{\vec{R}}_{01} + \sum_{i=1}^{N} M_i(\vec{\omega}_i \times \vec{r}_i) + \sum_{i=1}^{N} M_i\left(\sum_{k=2}^{i} \vec{\omega}_k \times \vec{\rho}_k\right) = 0 \tag{49}$$

which can also be expressed as

$$M\dot{\vec{R}}_{01} + \sum_{i=1}^{N} M_i(\vec{\omega}_i \times \vec{r}_i) + \sum_{i=2}^{N} \left(\sum_{k=1}^{N} M_k\right)(\vec{\omega}_i \times \vec{\rho}_i) = 0 \tag{50}$$

The vectors in (50) should be expressed in terms of their components in the same coordinate frame. Thus, we scalarize (50)

$$M\dot{\vec{R}}_{01} + \sum_{i=1}^{N} M_i \bar{C}_i^1 \cdot (\bar{\omega}_i \times \bar{r}_i) +$$

$$\sum_{i=2}^{N}\left(\sum_{k=1}^{N} M_k\right) \bar{C}_i^1 \cdot (\bar{\omega}_i \times \bar{\rho}_i) = 0 \tag{51}$$

where we have arbitrarily chosen the first body as the computational coordinate frame and the transformation matrices $\bar{C}_i^1$ are employed to transform the vectors $\vec{\omega}_i$, $\vec{r}_i$ and $\vec{\rho}_i$ expressed in the ith body coordinates, back to the first body coordinates. As an example, for 4-bodies in series (51) is used to find $\dot{\vec{R}}_{01}$.

23

$$-M\dot{\bar{R}}_{01} = M_1(\bar{\omega}_1 \times \bar{r}_1) + M_2\bar{C}_2^1 \cdot (\bar{\omega}_2 \times \bar{r}_2)$$
$$+ M_3\bar{C}_3^1 \cdot (\bar{\omega}_3 \times \bar{r}_3) + M_4\bar{C}_4^1 \cdot (\bar{\omega}_4 \times \bar{r}_4)$$
$$+ (M_2 + M_3 + M_4)\bar{C}_2^1 \cdot (\bar{\omega}_2 \times \bar{\rho}_2)$$
$$+ (M_3 + M_4)\bar{C}_3^1 \cdot (\bar{\omega}_3 \times \bar{\rho}_3) \tag{52}$$

(The $\bar{\rho}_1$ and $\dot{\bar{\rho}}_4$ terms are noted to be zero.) After $\dot{\bar{R}}_{01}$ is computed, the remaining $\dot{\bar{R}}_{0i}$ needed to complete the solution for the constraints are found from (47). These $\dot{\bar{R}}_{0i}$ are needed in the solution of the equations for momentum and motion which are computationally performed in each of the gimballed bodies respective coordinate frames and so they are scalarized in the ith frame. From (46), and (47) we obtain the scalarized result

$$\dot{\bar{R}}_i = \bar{C}_{(i-1)}^i \cdot \dot{\bar{R}}_{0(i-1)} + \bar{\omega}_i \times (\bar{\rho}_i + \bar{r}_i) \tag{53}$$

and from (46) and (48)

$$\dot{\bar{R}}_i = \bar{C}_1^i \cdot \dot{\bar{R}}_{01} + \bar{\omega}_i \times \bar{r}_i + \sum_{k=2}^{i} \bar{C}_k^i \cdot (\bar{\omega}_k \times \bar{\rho}_k) \tag{54}$$

Equation (53) is obviously simpler than (54) and so it is the preferred method of calculating the $\dot{\bar{R}}_i$ (i.e., in succession).

Figure 4 shows the block diagram representation for the solution of the $\dot{\overline{R}}_i$ terms in equation (19) for the ith body angular momentum term $\overline{H}_{Qi}$ using equations (51) and (53). It is noted in Figure 3 that the 4th and last body is assumed to have the same reference gimbal point as the 3rd body so that $\overline{R}_{04} = \overline{R}_{03}$. The first and last bodies in the chain in Figure 3 have only a single gimbal point and so their values for $\widehat{\rho}_i$ are zero or undefined.
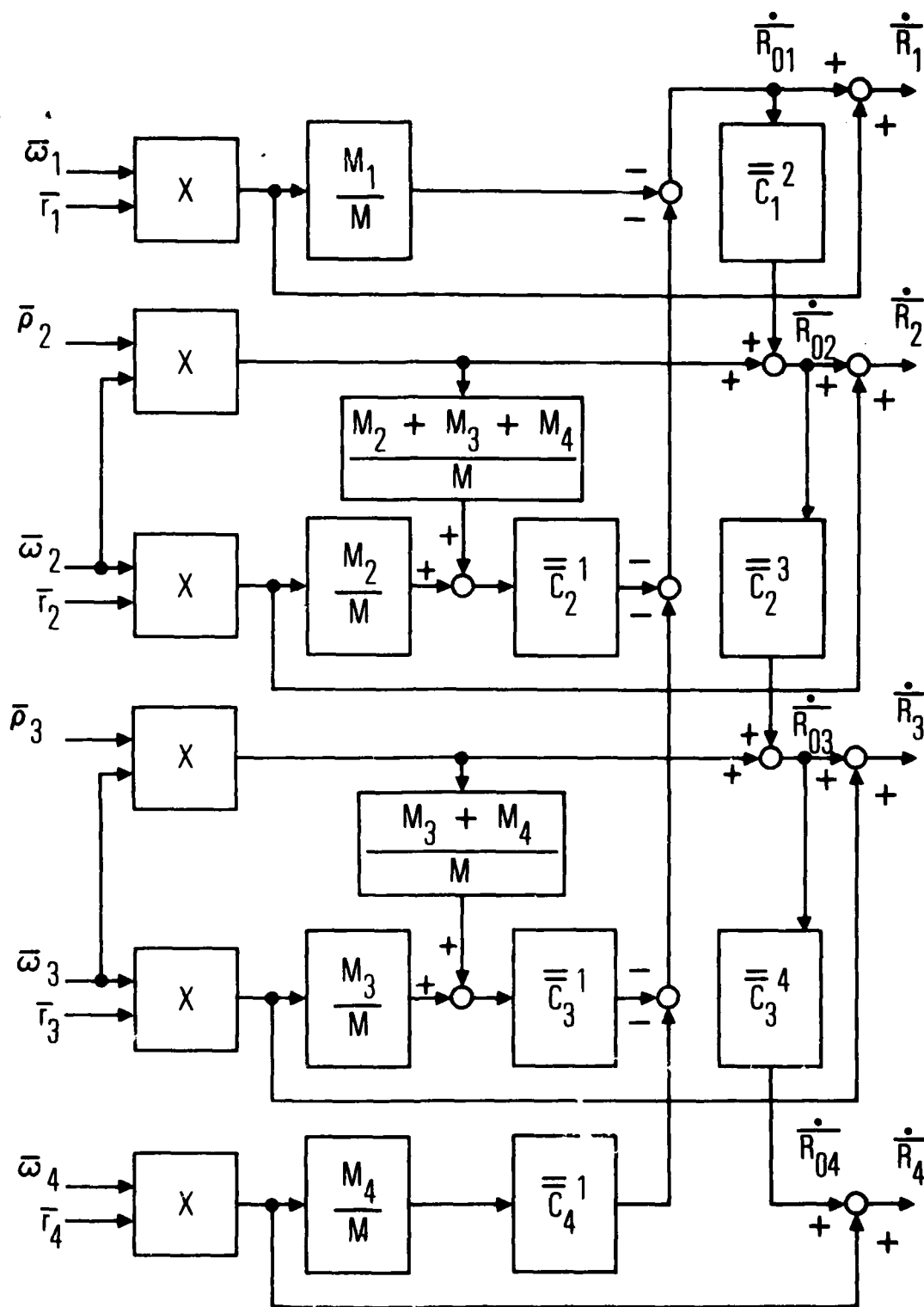
Figure 4. Momentum-Kinematic Constraints

26

5. ROTATIONAL MOTION RESTRAINT EQUATIONS

The solution of the equations of motion of a single body in the ensemble of bodies as depicted in Figure 2 can be carried out as previously noted using equations (18), (19), (28), (35), (51) and (53) yielding the body angular rates. The incremental angular motions that can be obtained by integration of the body angular rates, accounting for kinematics, are those angular motions about the gimballed i^{th} body G_i axes. Practically speaking, for gimbal motion freedom, one axis is unrestrained in the sense that large relative angular motion may occur (about the gimbal bearing axis) between the gimballed body and the neighboring body to which it is attached. The other two body axis motions relative to the attached body are restrained by the bearings to be small or near zero. One approach in writing simulation equations is to assume these transverse gimbal axes motions to be zero. This requires that "hard" constraint relations be solved algebraically in each integration step of the simulation. The analytical determination of the hard constraint relations is avoided in the approach taken here. Instead, the constraints for the bearing transverse axes are implemented by feeding back reaction torques about these axes that are proportional to small relative transverse axes angular motions. In effect then, the constraint relations appear as restraint gimbal stiffnesses. In fact, the stiffnesses used in the simulation can be the actual bearing transverse axes stiffnesses or perhaps the stiffnesses associated with the lowest frequency modes of vibration about these axes.

One can take the point of view that the so-called unrestrained axis or the bearing "free" axis is also restrained by the reaction and control torques relations for that axis. These torques include, for example, motor electromagnetic torque, motor cogging torque, motor magnetic hysteresis torque, bearing and motor solid friction torque, and viscous friction torque.

With these notions then, the transverse axes motions that would be oscillatory with stiffness feedback only, can also be dampened using realistic structural damping relations. If the simulation is expected to give good fidelity response data at the usually higher structural frequencies, the

27

damping introduced should be realistic. If the simulation is not expected to provide high fidelity results except at frequencies well below the structural frequencies, it is anticipated that high damping can be artificially introduced for the bearing transverse axis modes. This will allow the use of larger integration step sizes in a digital simulation and consequently will be more economical in computer run time. The restrained body dynamics equations are shown for the ith body in block diagram form in Figure 5.

Figure 5. Gimballed Body Restrained Dynamics

6. FOUR BODY SERVO SYSTEM EXAMPLE

6.1 GIMBALS/COORDINATES

An example of a multi-body gimbal servo system is illustrated in Figure 6. A block diagram of the "complete" dynamics equations for this example is shown in Figure 7.

The first body is the pointed experiment payload of mass M_1 which has a gimbal coordinate frame X_1, Y_1, Z_1 fixed in the payload with Z_1 along the line-of-sight of the experiment, X_1 is the cross-track gimbal axis, and Y_1 completes the triad. The center of mass of M_1 is offset from the G_1 gimbal center an amount $\bar{r}_1$.

The second body with mass M_2 is the gimbal yoke. The yoke gimbal center point G_2 is assumed to be midway between the cantilevered yoke bearings that provide free rotation of the yoke about the Y_2 axis. The yoke X_2 axis moves with the yoke and is parallel to the experiment X_1 gimbal axis. The Z_2 axis completes the yoke orthogonal frame. The center of mass of the yoke is offset from the G_2 gimbal point an amount $\bar{r}_2$.

The third body is the spacecraft and its gimbal frame G_3 is arbitrarily assigned to the same point as the solar array frame, G_4, i.e., it could also have been assigned to the same point as the yoke frame point G_2. As shown in Figures 4 and 6, the G_3 and G_4 points coincide. The spacecraft Y_3 axis is parallel to the yoke Y_2 axis and coincides with the solar array Y_4 axis. The spacecraft X_3 axis is fixed in the spacecraft parallel to one of its edges and also nominally parallel to the spacecraft orbital velocity vector. The Z_3 axis points in the direction of orbit nadir and completes the right handed triad.

The solar array X_4 axis is parallel to an edge of the array which is maintained normal to the sun line. The Z_4 axis completes the array frame G_4 triad.
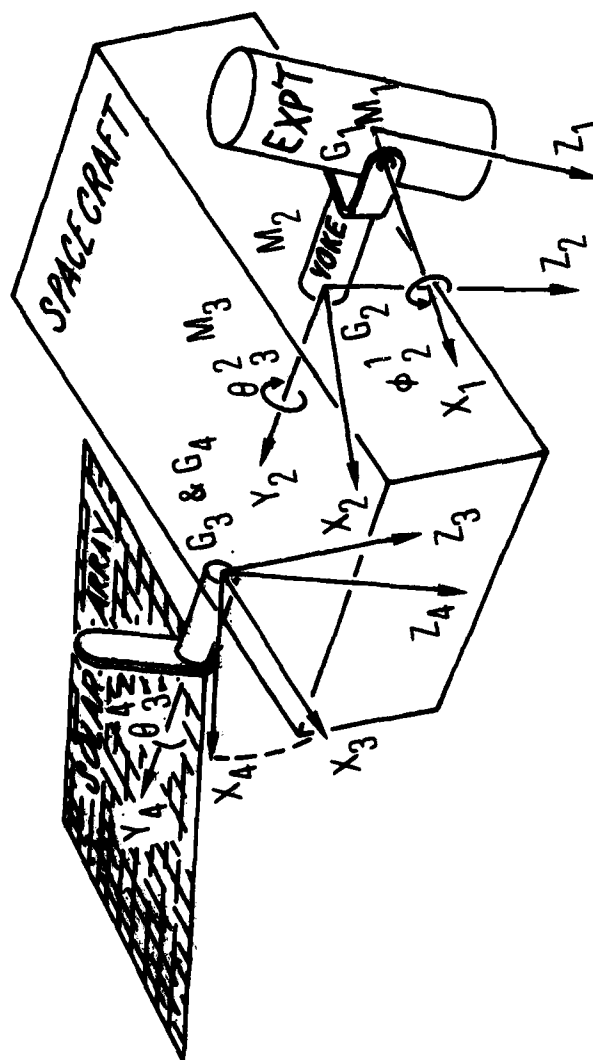
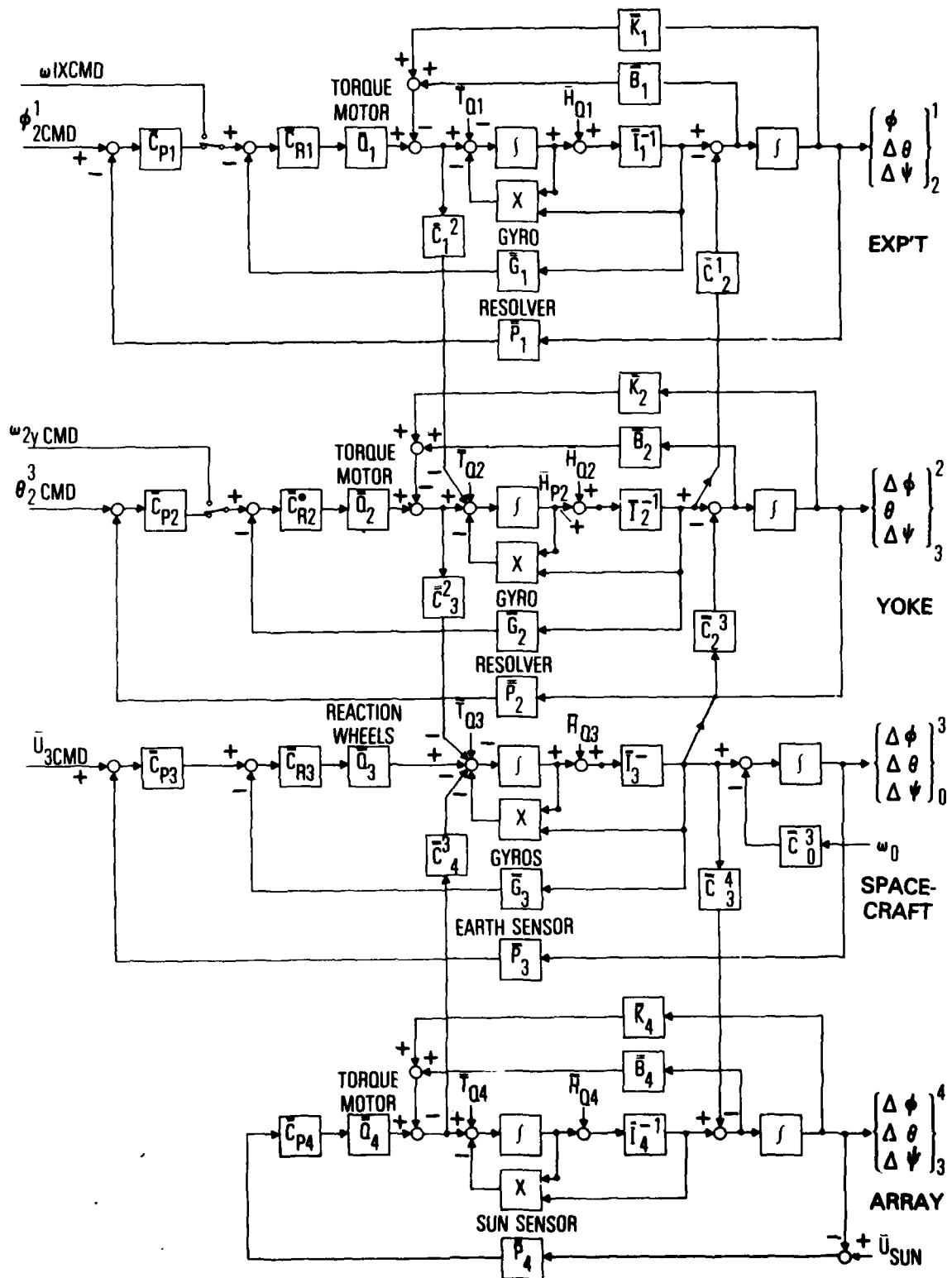Figure 6. Example of a Multi-Body Gimbal Servo System

Figure 7. Simulation Model for a Spacecraft With Gimballed Experiment and Solar Array

33

6.2   CONSTRAINTS AND RESTRAINTS

The constraint relations in Figure 4 apply to this example and in effect maintain the gimbal points geometry so that the distances between gimbals are maintained constant (e.g., $\vec{\rho}_2$ = vector from g_1 to g_2 = constant).

The "restraint" provisions that keep the angular rotation about the gimbal transverse axis small are the realistic stiffnesses about the experiment Y_1 and Z_1 axes, the yoke X_2 and Z_2 axes, and the solar array X_4 and Z_4 axes. The stiffnesses enter into the equations of restrained motion; for example, as indicated in Figure 5 for the ith body, and Figure 8 for the complete system, in the blocks labeled $\bar{\bar{K}}_1$ which are 3 × 3 stiffness matrices. The diagonal elements are the stiffnesses about the X_2, Y_2, Z_2 axes. The off-diagonal elements are assumed to be negligible. Since the yoke Y_2 axis is unrestrained except for solid friction, its stiffness is zero or small compared to the X_2 and Z_2 stiffness elements in $\bar{\bar{K}}_2$. Data for the stiffness elements can be obtained from design data or test data.

The other restraint provisions are applied somewhat realistically such as viscous friction in all axes in the $\bar{\bar{B}}_2$, 3 × 3, matrix in Figure 5. The diagonal elements are the viscous friction coefficients operating on the X_2, Y_2, Z_2 relative angular velocities. The off-diagonal terms are assumed negligible. The controlled Y_2 axis viscous friction coefficient can be found from test data. The X_2 and Z_2 axis friction coefficients can be assigned values that make the roots of the characteristic equation of the $\bar{\bar{I}}_2^{-1} K_2/s^2 +$ $\bar{\bar{I}}_2^{-1} B_2/S$ loops taken together for the X_2 and Z_2 channels overdamped such that the low frequency root is not much higher than the Y_2 control bandwidth (say for the rate control mode). If the undamped roots of the aforementioned characteristic equation lie within the control bandwidth, then an attempt should be made to use as realistic a friction model as possible for the transverse axes. Some viscous friction may be present for transverse axis motion of the gimbal axis relative to the adjacent spacecraft body through the action of lubrication as the viscous media. Perhaps a better choice of a model for incorporating damping is to use a simplified solid friction model[9] that results in realistic solid friction hysteretic damping. The model is an integral function of the relative angular rate $\Delta\omega_2$ given by

$$T_{Fj} = \int \sigma_j \left(1 - \frac{T_{Fj}}{T_{Cj}} \text{ sgn } \Delta\omega_{2j}\right) dt \tag{55}$$

where T_{Fj} is the j axis component of solid friction torque that retards the motion, σ_j is the solid friction model rest slope, and T_{Cj} is the coulomb friction torque level. Even though it is hysteretic, the model behaves like viscous friction for medium amplitudes of angular oscillatory motion but the behavior transitions to non-linear "structural damping" for very low amplitudes of oscillation. Structural damping virtually disappears near zero amplitude motion.

6.3   CONTROLLED AXES

The controlled gimbal axes are the experiment X_1 axis, the yoke Y_2 axis, and the solar array Y_4 axis.

6.4   SENSORS

Rebalance rate gyros (in $\bar{\bar{G}}_1$ and $\bar{\bar{G}}_2$ of Figure 7) are mounted with input axes along the X_1 and Y_2 axes and sense the inertial angular rates of the experiment and yoke about these axes. Angle pickoffs (in $\bar{\bar{P}}_1$ and $\bar{\bar{P}}_2$ of Figure 7) are also mounted on these axes and measure the relative Euler angles ϕ_2^1, θ_3^2. A sun sensor (in $\bar{\bar{P}}_4$) is mounted on the solar array and measures the angle between the sun vector and the Y_4Z_4 plane. An earth-sensor (in $\bar{\bar{P}}_3$) looks at the earth in the Z_3 direction and measures spacecraft pitch (about Y_3) and roll (about X_3) attitude errors. The spacecraft attitude control system also has rebalance rate gyros (in $\bar{\bar{G}}_3$) and a star sensor mounted on the spacecraft body (not shown in Figure 7).

6.5   ACTUATORS

The controlled gimbal axes are driven relative to the adjacent body by reacting against the adjacent body with D.C. torque motors. The spacecraft primary attitude control mode during experiment gimballing utilizes reaction wheels. The gimbal torque motor actuators are elements in the $\bar{\bar{Q}}_1$ and $\bar{\bar{Q}}_2$ blocks in Figure 7. The torque motor elements of $\bar{\bar{Q}}_i$ can be considered to be

Laplace transform transfer functions to account for dynamical effects of the torque motors if necessary. The spacecraft reaction wheels (not their housings) are actually additional bodies in the multi-body system and should be modelled like the other bodies. However, a simplification is justified if the reaction wheel momentum is small enough that it does not cause significant gyroscopic effects on the system. In this case, the reaction wheels can be considered to be devices which apply torque to the spacecraft through the dynamics of the wheel motor drive without the need to consider the effects of wheel speed on the system momentum. The wheels as torque generating devices are depicted in block $\bar{\bar{Q}}_3$ of Figure 7. The elements of the $\bar{\bar{Q}}_3$ matrix may be dynamics transfer functions.

6.6   COMPENSATION

The blocks labelled $\bar{\bar{C}}_p$ contain position control loop compensation transfer functions and the blocks labelled $\bar{\bar{C}}_R$ contain the rate control loop compensation transfer functions. In the case of the experiment, the ϕ and θ pointing position commands as well as the ω_{1x} and ω_{zy} rate commands are generated external to the control loops. Switchover from position to rate control is done to provide better tracking performance because of lower noise and higher loop bandwidth using the rate loop only. The usual proportional plus integral or proportional plus rate compensation is employed in the various compensators. The simplified diagram in Figure 7, for example, shows the solar array control without gyros or tachometer feedback and so proportional plus rate type compensation is used for this control loop.

7. SUMMARY

The equations of motion of a multi-body gimbal servo system for
simulation purposes were derived using a simplistic gimballed body momentum
formulation that was maintained throughout, thereby retaining the original
variables defined in the beginning of the model formulation. The avoidance of
unnecessary algebraic manipulation and the introduction of new variables
through transformation of the original variables is seen as a simplification
in evolving and understanding a complex computer simulation model that can be
debugged and run with enhanced insight to the physical process being
simulated.

One of the features that helped in this goal was the choice of writing
the equations of rotational motion in the body fixed coordinates of the
gimballed bodies. The result is the simple body rotational dynamics equation
diagram of Figure 2. The $\vec{r}_Q \times M\dot{\vec{R}}_Q$ moment of momentum term that is added to the
body rotational angular momentum is determined algebraically by evaluating the
gimbal interbody forces and utilizing conservation of translational momentum
in order to avoid solution of the translational dynamics. Although somewhat
involved, this process seems to evolve to solutions that are straightforward
as indicated by Figure 4.

The equations of rotational motion are expressed in the gimballed body
coordinates and thereby require fairly extensive transformation of angular
rates and torques from adjacent bodies, but this is true of other formulation
approaches. When a generalized coordinate approach to formulation is taken,
the coordinate transformations are hidden or essentially replaced by velocity
and momentum transformations. Thus, in this regard, there appears to be no
great disadvantage in the approach taken in this paper. However, there seems
to be an advantage in keeping the avenues of insight open by retaining the
original coordinate transformations throughout.

The equations necessary for the simulation of a 4-body system were
presented in matrix-scalar block diagram form in Figures 4 and 7. The
elements of the 3 × 3 matrices or dyadics need to be defined whereby it will

37

be found that many are zero and many are Laplace transform transfer functions. The component scalar equations are too detailed to devote additional attention in this report.

REFERENCES

1. Jerkovsky, W., "The Structure of Multi-Body Dynamics," AIAA Journal of Guidance and Control, Vol. 1, No. 3, 1978.

2. Russell, W. J., "On the Formulation of Equations of Rotational Motion for an N-Body Spacecraft," TR-0280(4133)-2, 1969, Aerospace Corp., El Segundo, CA.

3. Kane, T. R., & Levinson, D. A., "Formulations of Equations of Motion of Complex Spacecraft," AIAA Journal of Guidance and Control, Vol. 3, No. 2, 1980.

4. Jerkovsky, W., "The Transformation Operator Approach to Multi-Body Dynamics," TR-0076(6901-03)-5, 1976, Aerospace Corp., El Segundo, CA.

5. Wittenburg, J., Dynamics of Systems of Rigid Bodies, B. G. Teubner, Stuttgart, Germany, 1977.

6. Thompson, W. T., Introduction to Space Dynamics, John Wiley, New York, NY, 1961.

7. Goldstein, H., Classical Mechanics, Addison-Wesley, Reading, Mass, 1959.

8. Likens, P. W., Elements of Engineering Mechanics, McGraw Hill, New York, NY, 1973.

9. Dahl, P. R., "Solid Friction Damping of Mechanical Vibrations," AIAA Journal, Vol. 14, No. 12, 1976.

APPENDIX A

1. <u>SCALARIZING</u>

The vector equations in this paper are used in vector-dyadic form until
the need arises to scalarize into matrix-scalar forms. For computer time
history simulations, we need the matrix-scalar form as an end product to work
from and the block diagrams used herein are in that form. In scalarizing, the
assumption is made that a vector $\vec{R}$ can be written in terms of its components
along some bases $\hat{u}_{Ax}$, $\hat{u}_{Ay}$, $\hat{u}_{Az}$. In vector form,

$$\vec{R} = \overline{R}_A \hat{u}_A = R_{Ax}\hat{u}_{Ax} + R_{Ay}\hat{u}_{Ay} + R_{Az}\hat{u}_{Az} \tag{A-1}$$

Then alternatively in matrix-vector form

$$\vec{R}_A = \{R_A\} = [R_{Ax}, R_{Ay}, R_{Az}]\{\hat{u}_{Ax}, \hat{u}_{Ay}, \hat{u}_{Az}\}^T \tag{A-2}$$

$$= [R_A]\{\hat{u}_A\} \tag{A-3}$$

$$= \begin{bmatrix} R_{Ax}\hat{u}_{Ax} \\ R_{Ay}\hat{u}_{Ay} \\ R_{Az}\hat{u}_{Az} \end{bmatrix} \tag{A-4}$$

or in terms of its scalar components in frame <u>A</u> the matrix-scalar form is

$$\overline{R}_A = [R_A] = \begin{bmatrix} R_{Ax} \\ R_{Ay} \\ R_{Az} \end{bmatrix} \tag{A-5}$$

41

The idea of a matrix such as the component matrix $[R_A]$ operating on a vector $|\hat{u}_a|$ producing a "transformed" vector $\left[R_A\right]_B$ is applied to coordinate transformations where a rotation matrix $[C_A^B]$ operating on a vector say $\vec{S}_A$ produces a vector $\vec{S}_B$. In "matrix vector" form,

$$\{S_B\} = [C_A^B] \ \{S_A\} \tag{A-6}$$

or

$$\begin{Bmatrix} S_{Bx}\hat{u}_{Bx} \\ S_{By}\hat{u}_{By} \\ S_{Bz}\hat{u}_{Bz} \end{Bmatrix} = [C_A^B] \begin{Bmatrix} S_{Ax}\hat{u}_{Ax} \\ S_{Ay}\hat{u}_{Ay} \\ S_{Az}\hat{u}_{Az} \end{Bmatrix} \tag{A-7}$$

and in matrix-scalar form

$$\{S_B\} = [C_A^B] \ \{S_A\} \tag{A-8}$$

or

$$\overline{S}_B = [C_A^B] \ \overline{S}_A \tag{A-9}$$

or

$$\begin{bmatrix} S_{Bx} \\ S_{By} \\ S_{Bz} \end{bmatrix} = [C_A^B] \begin{bmatrix} S_{Ax} \\ S_{Ay} \\ S_{Az} \end{bmatrix} \tag{A-10}$$

The vector dyadic form

$$\vec{S}_B = \bar{\bar{C}}_A^B \cdot \vec{S}_A \tag{A-11}$$

is represented in matrix scalar form as

$$\overline{S}_B = \overline{\overline{C}}{}_A^B \cdot \overline{S}_A \tag{A-12}$$

where the dyadic and matrix $\overline{\overline{C}}{}_A^B$ are equivalent.

The vector $\vec{R}$ in (A-1) and (A-3) did not have to be identified with respect to a coordinate frame until its components needed to be known, at which time its bases $\hat{u}_{AX}$, $\hat{u}_{AY}$, $\hat{u}_{AZ}$ have to be specified. In the case of the coordinate transformation, (A-6), the bases of $\vec{S}$ were presumably known to be in frame A before the transformation matrix or dyadic $\overline{\overline{C}}{}_A^R$ could be generated to produce that vector's components in the B frame. In this sense, the "matrix vector" form is already in a scalarized form by identifying the A and B frame bases vectors.

2.   DERIVATIVES

If a vector derivative operation is required in a fixed inertial frame with bases u_{Ax}, u_{Ay}, u_{Az}, the components of $\vec{R}$ are identified from

$$\dot{\vec{R}} = \dot{\overline{R}}_A \hat{u}_A = \dot{R}_{Ax}\hat{u}_{Ax} + \dot{R}_{Ay}\hat{u}_{Ay} + \dot{R}_{Az}\hat{u}_{Az} \tag{A-13}$$

wherein the scalar components are seen to be

$$\dot{\overline{R}}_A = \begin{bmatrix} \dot{R}_{Ax} \\ \dot{R}_{Ay} \\ \dot{R}_{Az} \end{bmatrix} \tag{A-14}$$

If the components of a vector derivative of $\vec{R}$ are known in a frame B rotating at an inertial angular rate $\vec{\omega}$ with respect to an inertial frame A, the components of the vector derivative in the inertial frame can be found from the vector formula

$$\dot{\vec{R}}_A = \dot{\vec{R}}_B + \vec{\omega} \times \dot{\vec{R}}_B \tag{A-15}$$

43

They are the corresponding quantities of the matrix scalar equation,

$$\dot{\overline{R}}_A = \dot{\overline{R}}_B + \overline{\omega}_B \times \dot{\overline{R}}_B \tag{A-16}$$

where the symbols $\overline{\omega}x$ denotes a 3×3 skew-symmetric matrix operator that operates on the 1×3 column matrix $\dot{\overline{R}}_B$ i.e.,

$$\omega_B \times = \begin{bmatrix} 0 & -\omega_{Bz} & \omega_{By} \\ \omega_{Bz} & 0 & -\omega_{Bx} \\ -\omega_{By} & \omega_{Bx} & 0 \end{bmatrix} \tag{A-17}$$

Sometimes the components of a vector derivative $\dot{\vec{R}}$ (or any vector for that matter) are known in an inertial frame A and it is desired to determine its components in another frame B which may be rotating or not. Here, the components of $\dot{\vec{R}}$ in the frame B are [see (A-12)]

$$\dot{\overline{R}}_B = \overline{\overline{C}}_A^B \cdot \dot{\overline{R}}_A \tag{A-18}$$

It perhaps should be pointed out that $\vec{\omega}$ in (A-15) is the inertial angular velocity of the B frame whose components, if need be, can be transformed via formula (A-12)

$$\overline{\omega}_B = \overline{\overline{C}}_A^B \cdot \overline{\omega}_A \tag{A-19}$$

All of the vectors on the right side of (12) are thereby scalarized in (17) to the same reference frame. Note that if there is more than one subscript to a scalar 1×3 matrix, the last subscript denotes the reference frame, e.g., $\overline{\omega}_{23}$ indicates the scalar components of $\vec{\omega}_2$ are in frame 3.

3. TRANSFORMATIONS

The transformation matrix $[C_A^B]$ or dyadic $\bar{\bar{C}}_A^B$ can be a single or multiple axis Euler angle transformation. Here, for single Euler angle rotation transformations,

$$[\phi_A^B] = \begin{bmatrix} 1 & 0 & 0 \\ 0 & C\phi & S\phi \\ 0 & -S\phi & C\phi \end{bmatrix} , \qquad\qquad \text{(A-20)}$$

which is a ϕ rotation about X_A axis in the sequence to get to B frame,

$$[\theta_A^B] = \begin{bmatrix} C\theta & 0 & -S\theta \\ 0 & 1 & 0 \\ S\theta & 0 & C\theta \end{bmatrix} , \qquad\qquad \text{(A-21)}$$

is a θ rotation about Y_A axis in the sequence to get to B frame, and

$$[\psi_A^B] = \begin{bmatrix} C\psi & S\psi & 0 \\ -S\psi & C\psi & 0 \\ 0 & 0 & 1 \end{bmatrix} , \qquad\qquad \text{(A-22)}$$

is a ψ rotation about Z_A axis in the sequence to get to the B frame, where X_A, Y_A, Z_A are the axes of the G_A frame. If a gimbal axis set, through which gimbal Euler angles occur, has zero or negligible mass and inertia, and are intersecting, then the transformation (19) can be taken as the product of successive rotational transformations of the massless gimbal set. For example, if the massless gimbal set order of rotation is, first about X_A,

second about Y_A, and third about Z_A, then to get from the G_A frame to the G_B gimbal frame,

$$\overline{C}_A^B = \overline{\psi}_A^B \cdot \overline{\theta}_A^B \cdot \overline{\phi}_A^B \tag{A-23}$$

In the usual case where a gimbal has appreciable or finite mass, and a single bearing axis is employed which may be non-intersecting with other gimbals, then that gimbal should be considered as a separate body and a single angle rotation (about the gimbal axis) transformation is deemed adequate. However, strictly speaking, the small angle rotations about the axes transverse to the bearing axis which can be considered co-centered should be included in the general 3-axis case as in Equation (A-23).

4.   ATTITUDE KINEMATICS

The gimbal or body angles or parameters that characterize the attitude of the body are computationally obtained from kinematics rate equations. In the case of Euler angles that are used in this paper they are obtained by integration of kinematic rate equations typically of the form

$$\begin{bmatrix} \dot{\phi} \\ \dot{\theta} \\ \dot{\psi} \end{bmatrix} = \begin{bmatrix} 1 & \dfrac{S\theta S\phi}{C\theta} & \dfrac{S\theta C\phi}{C\theta} \\ 0 & C\phi & -S\phi \\ 0 & \dfrac{S\phi}{C\theta} & \dfrac{C\phi}{C\theta} \end{bmatrix} \begin{bmatrix} \omega_X \\ \omega_Y \\ \omega_Z \end{bmatrix} \tag{A-24}$$

Where the order of Euler angle rotation here is yaw-pitch-roll (i.e., 1st about Z, 2nd about Y, 3rd about X). The coefficient matrix is non-orthogonal for Euler angle transformations and possesses singularities. The singularity condition is avoided for small angle rotations transverse to the gimbal axis if the first rotation in the sequence is taken to be the gimbal bearing axis. Also, the coefficient matrix is then independent of the bearing axis Euler angle. Thus, if small angle approximations for pitch, θ, and

46

roll, ϕ, are used, which represents the small angular deflections transverse
to the bearing Z axis, we get for the above example,

$$\begin{bmatrix} \dot{\phi} \\ \dot{\theta} \\ \dot{\psi} \end{bmatrix} = \begin{bmatrix} 1 & 0 & \theta \\ 0 & 1 & -\phi \\ 0 & \phi & 1 \end{bmatrix} \begin{bmatrix} \omega_X \\ \omega_Y \\ \omega_Z \end{bmatrix} \qquad (A-25)$$

where, again, it is seen that the coefficient matrix does not contain the
bearing axis rotation angle, ψ.

It may easily be ascertained that the small angle approximation for the
coefficient matrix is not unique and independent of the order of the last two
rotations, i.e., pitch-roll vs. roll-pitch. This observation and the
assumption that the transverse axis rotations will be truly small and
oscillatory, are motivations for setting the small angles in the coefficient
matrix to zero. The coefficient matrix is then seen to be the identity
matrix.

The spacecraft attitude errors are obtained in a similar fashion,
however the attitude errors are referenced to the local orbit frame. Thus,
the attitude kinematic rate equations are of the form of equation (A-24)
except the rate error vector on the right side of equation (A-24) is

$$\Delta \bar{\omega} = \bar{\omega}_3 - \bar{C}_0^3 \, \bar{\omega}_0 \qquad (A-26)$$

which is reflected in Figure 7 as the spacecraft attitude error rate.

DA
FILI
3